Sim Biology- Driven PK–PD Modeling of Exosome (miR-378) Delivery to Reduce Collagen Overproduction in Cardiac Fibrosis

Arnav Guduri*

Austin Community College, United States

***Corresponding Author**
Arnav Guduri, Austin Community College, United States.

Citation: Guduri, A. (2025). Sim Biology- Driven PK–PD Modeling of Exosome (miR-378) Delivery to Reduce Collagen Overproduction in Cardiac Fibrosis. *Ope Acce Jou Dis Glo Heal, 3*(3), 01-10.

Abstract
Cardiac Fibrosis lacks consistent and reliable treatment utilizing drugs such as ACE inhibitors, coagulants, and ARBS. As modeling and simulation are increasingly used in drug development to understand pharmacokinetic-pharmacodynamic (PK-PD) relationships and support preclinical research, I simulate an extracellular vesicle (EV), an exosome modified with miR378, to reduce collagen buildup that causes Cardiac Fibrosis (CF) in the cardiac interstitium. Using the Simbiology® graphical user interface (GUI), I perform a bolus dose, a pulsed dose, and a binding + maintenance dose. I demonstrated presentational pathway figures, parameters, species estimation, and thermodynamic binding affinities. The results show that bolus and multiple-pulse doses are highly effective at stopping fibrotic collagen production in the interstitial space.

Keywords: PK-PD, Cardiac Fibrosis, Exosomes, Mir378, Collagen

1. Introduction
CF, characterized by collagen turnover in the cardiac interstitium a condition, can lead to heart failure (HF), arrrhytmias and myocardial infarctions. A study by Gulati et al. with 142 participants reported that there was a 26.8% increase in death rate for patients with midwall fibrosis compared to the death rate of 10.8% of patients without fibrosis after a 5.3-year check-up [1]. Another study found that cardiac remodeling induced by the onset of fibrosis has a death rate of 8% in patients > 75 years of age [2]. The WHO has predicted that by 2008, with 17.3 million deaths from cardiovascular disease, this will increase to around 25 million deaths per year, meaning that an average of 2150 Americans die from CVD every day [3]. With cardiac fibrosis being a very common condition that leads to remodeling, hypertension, infarctions, and many other heart conditions, there still seems to be a lack of appropriate, authenticated care targeting one of the primary causes of collagen overproduction. Many studies have diagnosed that these heart conditions are caused by collagen overproduction and subsequently perturbation of regulating complexes [4]. However, there is very limited treatment and research that targets collagen directly. Currently, options are ACE inhibitors, beta-blockers, and experimental anti-TGF-β therapy. MicroRNA treatment has begun to emerge, but it is relatively new in the field of heart conditions.

### 1.1. Collagen Structure, Purpose and Production Pathway
Collagen (either COL1, COL2, or COL3) is an extracellular matrix (ECM) protein that is integral to the structure of several parts of our body, from skin to muscles and bones. Collagens I and III are critical to maintaining tissue architecture and the geometry of the myocardium chamber. It is an integral component of connective tissue and is metabolically active due to fibroblasts. However, its overexpression has negative implications. Excess synthesis causes stiffening of the heart, affecting diastolic and systolic function, leading to a wide variety of conditions such as atrial fibrillation (AF), fibrosis, and heart failure [5]. The focus of this paper is on the expression of collagen through fibroblasts. In cardiac tissue, there are a few main components, namely fibroblasts, myocytes, and capillaries (Fig 3).

Cardiac tissue is not uniform, as it consists of different microenvironments with anatomy and cellular composition depending on the location of the heart tissue, so for this model, atrial cardiac tissue [6]. Within the CI is an important complex called the MMP-TIMP1 Complex. In this complex, Matrix Metalloproteinases (MMPs) degrade ECM proteins that aren't needed for the regulatory function of the cardiac tissue, and the TIMP (Tissue-Inhibitor of Metalloproteinases) regulates the activity of MMPs along with a pathway called the TGF-β pathway [7]. Fibroblasts are the main producers of collagen, and it is important to understand the process of collagen production to understand the purpose of miR-378. The fibroblast TGF-β1-Signaling Pathway is responsible for the production of collagen as a response to the necessities of heart tissue repair.
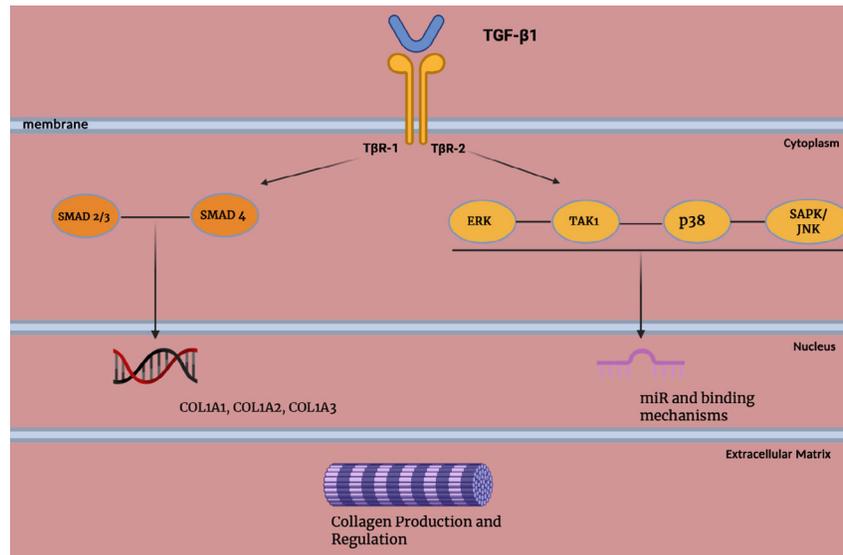
Figure 1: TGF-β ligand binds to its dimerized receptors TβI and TβII which activates 3 sub-pathways that contribute to regulation and production of collagen. This computational model focuses on the SMAD 2/3/4 phosphorylation cascade. SMAD 2/3 binds with SMAD 4 (co-SMAD) leading to nucleus translocation subsequently intiating protein synthesis. The other pathways [8]. The other pathways contribute to miR pathways and regulatory complexes [9-11,7]
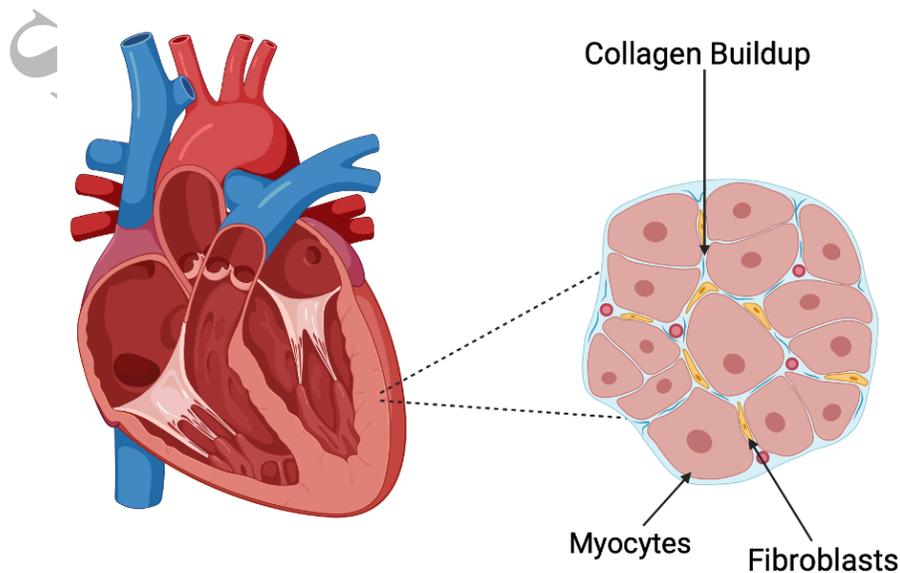
Figure 2: This diagram illustrates the anatomy of cardiac tissue. Within the membrane of this tissue lie 3 main components that play an active role in this model, which are myocytes, fibroblasts, and cardiac interstitium (CI), which is the space between myocytes where fibroblasts and protein producers lie [12]

Collagen production is essential for the proper functioning and structure of heart organs and tissue; however, its overexpression has negative implications. The excess synthesis of collagen can disrupt the structure and function in several ways. The myocardium of the heart stiffens, resulting in a consequentially negative impact on diastolic and systolic function, leading to impaired blood flow. Another effect is hypertrophy of the heart where myocytes begin to thicken and grow abnormally. This can lead to a multitude of conditions such as atrial fibrillation, cardiac fibrosis, and heart failure [3]. However, in cardiac tissue cells there is a specific miRNA called miR-378 which is responsible for the regulation of collagen synthesis that is integral to the delivery method of this experiment. During normal conditions, there is an abundant amount of miR-378 which prevents collagen gene expression by functioning as its miRNA job by blocking the translation of these genes into proteins. However, due to conditions, an excessive abundance of collagen reduces the expression of miR-378, which leads to even more collagen production leading to the heart conditions mentioned above.
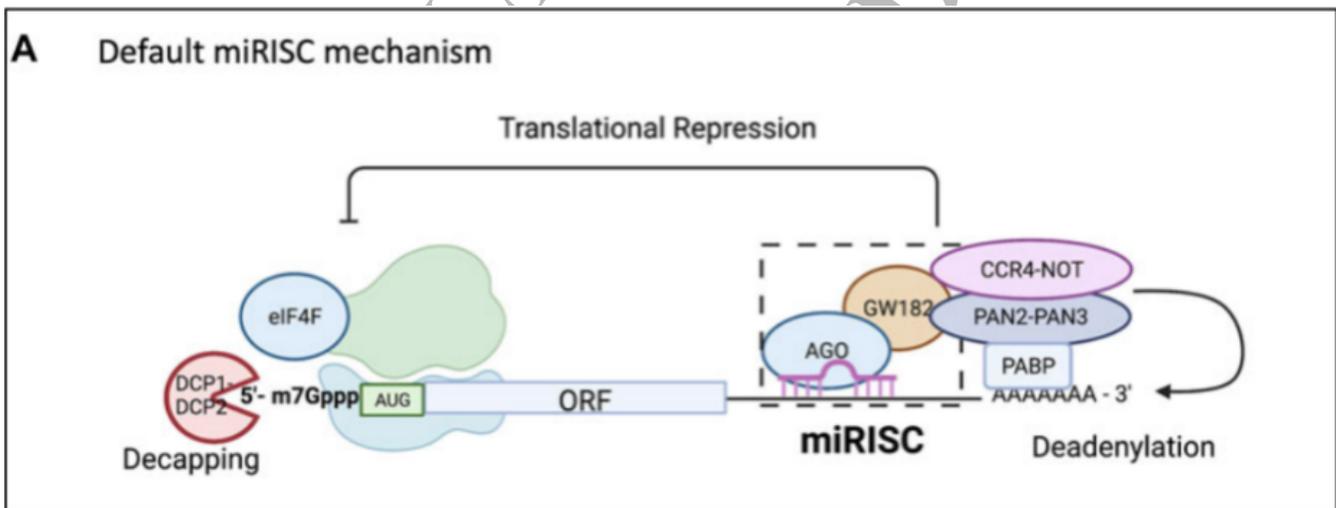
1.2. Mir378

miR-378, 22, 218-5p, 363-3p, 1246, 1290, and 126 are all present, but miR-378 is most abundant and most directly purposeful for anti-fibrotic effects. Yuan et al state that in a knockout mouse model, miR378 utilizes the P38 MAPK signaling pathway linked to cardiac remodeling, working with the MMPs and collagen in fibroblasts. Through this function, miR378 significantly reduces the extensive mechanical tissue stretching of COL2A1 and COL1A1 [10]. The overall characteristics of miR378 are available through its mechanistic function of binding to collagen mRNA 3'-UTRs, destroying it before translation with the addition of the deadenylase complex (Fig 4) [13].

1.3. Exosomes

The exosomes are 30–200nm in size, allowing the breach of smaller cell barriers. Additionally, they are extremely biocompatible and robust, characterized by their rigid lipid bilayers, low immunogenicity, reduction of toxicity, and bypass of lysosomal degradation. This EV is viable for analysis tracking through chromatography and nanoparticle tracking analysis as well. Their main anatomical feature for drug delivery is the CD63 tetraspanin surface protein. Attracted to rich areas of TIMP1 within the cardiac interstitium, miR378 is more viable to deliver accurately [3].

Figure 3: This diagram illustrates the process of miR378 reducing collagen expression: the ElF4F complex (not a part of miRs) recruits ribosomes to induce the process of translation of collagen mRNA which is when GW182 is recruited which brings CCR4-NOT and PAN2PAN3 which are the dead enylase complexes that work together to break down the poly-A tail of mRNA paired along with DCP1/DCP2 which destroys the 5' end of the strand [13]

2. Methodology
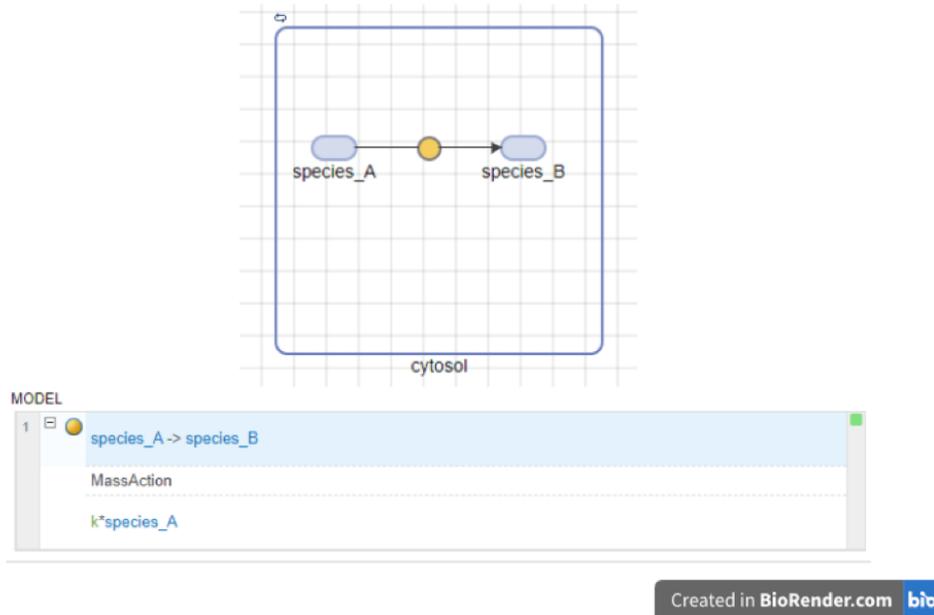
Figure 4: Sample reaction in Simbiology® paired with ODE. The diagram represents species A as a reactant that leads to the product of species B. Along with this reaction is paired a Mass Action ODE with a parameter of "k" that controls the rate of production of species B

2.1. PK-PD Compartment Development

A PKPD model was developed to represent the intravenous injection of exosomes into the bloodstream that travels to the myocardial tissue barrier subsequently permeating within the CI after entry and disperse miR378 to act according to its function [14].

The pharmacological parameter of exosome uptake is calculated and fitted from HDock® following the collagen synthesis via the TGF-B pathway in its production site of fibroblasts that lie within the CI. miR378 mechanistic functions simultaneously intervene collagen synthesis within this model.
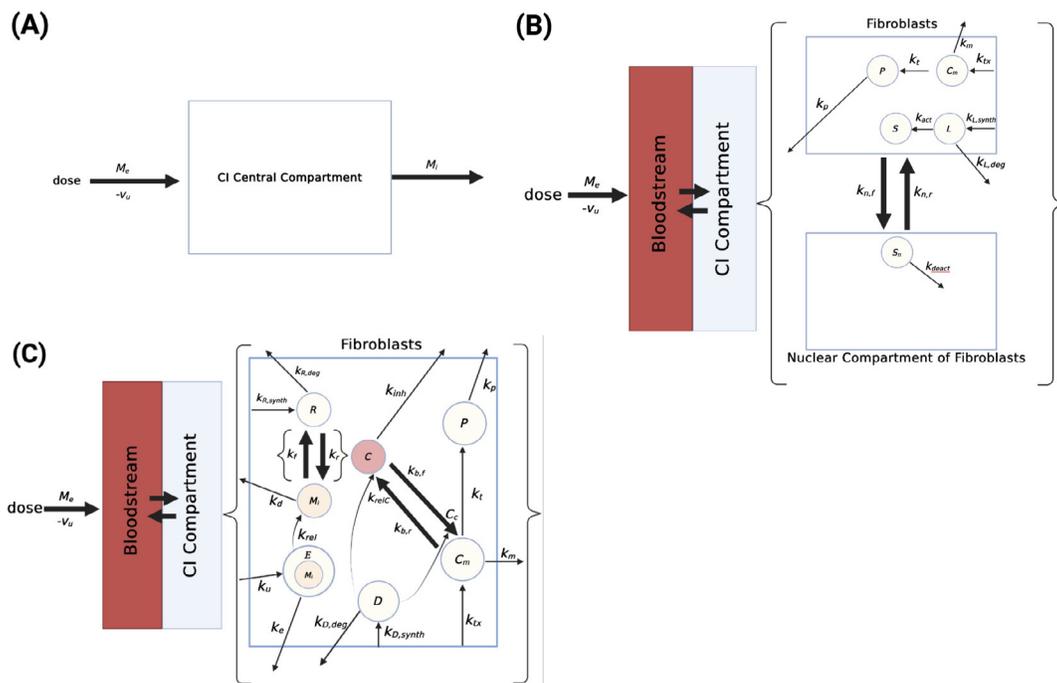
Figure 5: (A) is general drug delivery workflow; (B) is TGF-β induced collagen synthesis; (C) is miR378 cleaving mechanisms omitting TGF-β ligand production.

2.1.1. Exosome Uptake ODE

$$\frac{dM_e}{dt} = -v_u \cdot M_e$$

v_u is the uptake rate of exosomes entering the cytosol from drug central via permeation of the capillary wall, which was calculated with H Dock®—thermodynamic values of CD63TIMP1. Exosomes are a nanotechnology for delivery and M_e are the species of miR-378 extracellularly.

2.1.2. Development of Mir378 Mechanisms

Within the cardiac interstitium, primarily as a basis for collagen synthesis in fibrotic conditions, is separated by the capillary wall. After the uptake of exosomes into the CI, intricate modeling of the deadenylase complex formation, degradation measures, miRISC complex formation, and binding to collagen mRNA are explicitly modeled to describe miR378 processes. Along with these processes is the TGF-β pathway that occurs in fibroblasts, which induces collagen production. It translates to the nucleus of fibroblasts, additionally, in order to begin the transcription process of collagen.

$$\frac{dM_i}{dt} = k_{\text{rel}}E - k_f M_i R + k_r C - k_d M_i$$

$$\frac{dC_m}{dt} = k_{b,f} \cdot C C_m + k_{b,r} C_c - k_m C_m - k_t C_m + k_{\text{tx}} S_n$$

$$\frac{dR}{dt} = k_{R,\text{synth}} - k_{R,\text{deg}}R - k_f \cdot M_i \cdot R + k_r C$$

$$\frac{dC}{dt} = k_f \cdot M_i R - k_r C - k_{b,f} \cdot C \cdot C_m + k_{b,r} C_c + k_{\text{relC}} C_c$$

$$\frac{dC_c}{dt} = k_{b,f} \cdot C \cdot C_m - k_{b,r} C_c - k_{\text{inh}} C_c - k_{\text{relC}} C_c$$

$$\frac{dD}{dt} = k_{D,\text{synth}} - k_{D,\text{deg}}D + k_{\text{relC}} \cdot C_c$$

2.1.3. Development of Collagen Synthesis and Regulation ODEs

$$\frac{dP}{dt} = k_t \cdot C_m - k_p P$$

$$\frac{dS}{dt} = k_{\text{act}}L - k_{n,f} \cdot S + k_{n,r} \cdot S_n$$

$$\frac{dL}{dt} = k_{L,\text{synth}} - k_{L,\text{deg}} \cdot L - k_{\text{act}}L$$

$$\frac{dS_n}{dt} = k_{n,f}S - k_{n,r} \cdot S_n - k_{\text{deact}}S_n$$

2.1.4. Exosome Degradation within CI

$$\frac{dE}{dt} = k_u M_e - k_e E$$

Symbol	Meaning
M_e	Exosomal miR-378 concentration
M_i	Intracellular miR-378 concentration
R	Free AGO2
C	miR-378:AGO2 complex (miRISC)
C_m	Collagen mRNA
C_c	Collagen mRNA bound to miRISC
P	Collagen I protein
E	Internalized exosomes
D	Deadenylase complex
L	TGF-β ligand
S	Cytoplasmic active SMAD complex
S_n	Nuclear active SMAD complex
k_u	Exosome uptake rate
k_e	Exosome degradation rate
k_{rel}	miR-378 release rate from internalized exosomes
k_f	miRISC formation forward rate constant
k_r	miRISC dissociation reverse rate constant
$k_{b,f}$	miRISC binding to collagen mRNA (forward)
$k_{b,r}$	miRISC unbinding from collagen mRNA (reverse)
k_{relC}	Release of miRNA from collagen mRNA complex
k_{inh}	Rate of mRNA–miRISC degradation

k_t	Collagen translation rate
k_p	Collagen protein degradation rate
k_m	Collagen mRNA basal degradation rate
k_{tx}	Collagen transcription rate
$k_{R,\text{synth}}$	AGO2 synthesis rate
$k_{R,\text{deg}}$	AGO2 degradation rate
$k_{D,\text{synth}}$	Deadenylase synthesis rate
$k_{D,\text{deg}}$	Deadenylase degradation rate
$k_{L,\text{synth}}$	TGF-β ligand generation rate
$k_{L,\text{deg}}$	TGF-β ligand degradation rate
k_{act}	Ligand–Receptor mediated SMAD activation rate
$k_{n,f}$	SMAD nuclear translocation forward rate
$k_{n,r}$	SMAD nuclear translocation reverse rate
k_{deact}	Nuclear SMAD complex deactivation rate
k_d	Intracellular miR-378 degradation rate

Table 1: ODE Symbol Biological Meaning in Model

2.2. Biophysical Parameter Estimations
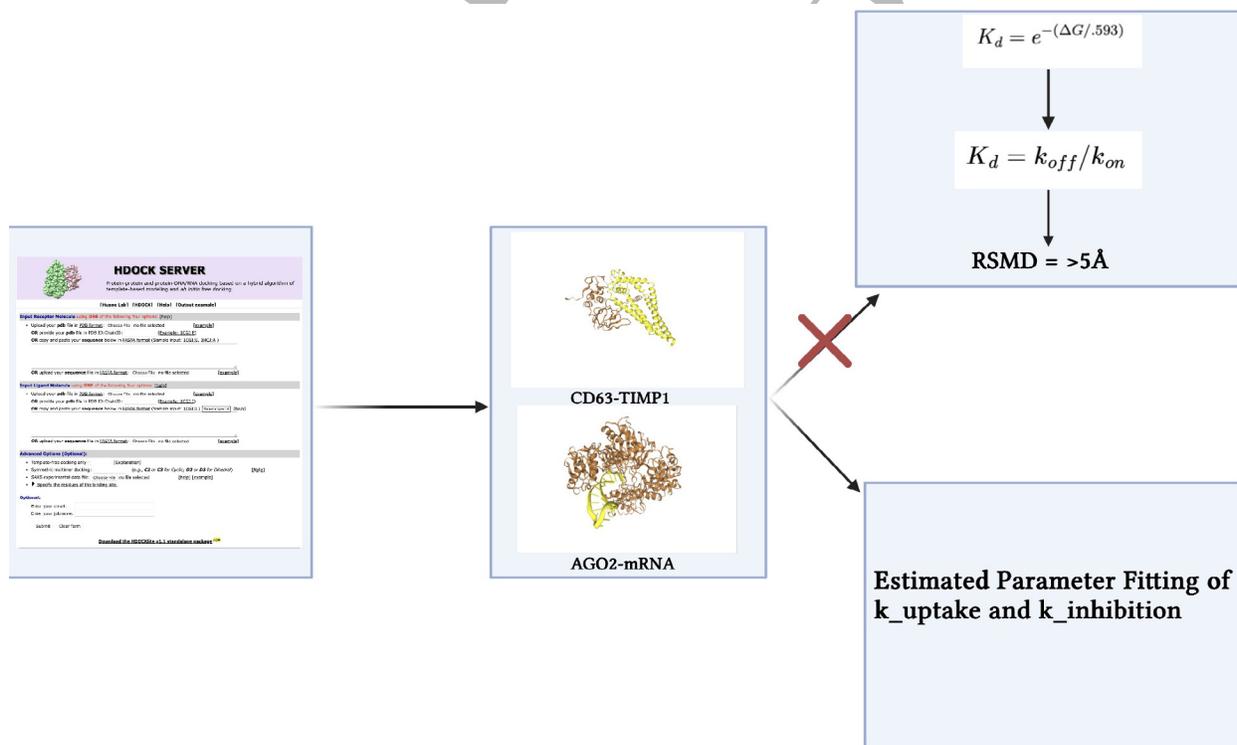
Figure 6: k_{uptake} and $k_{inhibition}$ workflow: The HDock server's input PDB fields were used for ligand and receptor for either of the CD63-TIMP1 or AGO2-COl1 mRNA. After simulation the most accurate model consists of the lowest RSMD in units of angstroms (˚A). The value in J mol is calculated into a K_d dissociation constant value that is then put into the $K_d = k_{off}/k_{on}$ equation (view Figure 6 for derivation and calculations). However affinity values were disregarded due to a RSMD greater than 5˚A and k_{off} values were too high causing integration errors in Simbiology. Thus, rescaling fitting was implemented into values of 3262 1/hour for k_{uptake} and 17 1/hour for $k_{inhibition}$ based off original values of -267.50 Jmol for AGO2-COL1 mRNA and -314.57 Jmol for CD63-TIMP1 [15-19].
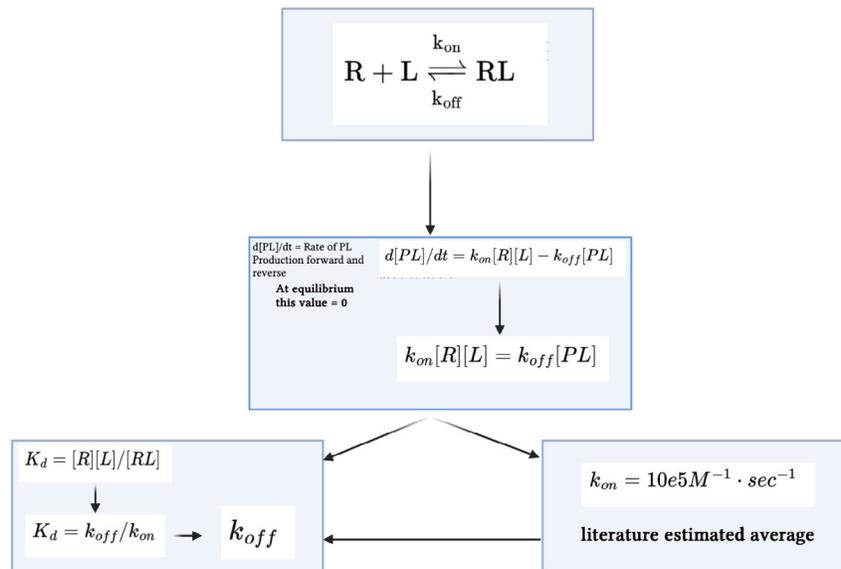
Figure 7: R represents receptor and L represents ligand. This kinetics equation with k_{on} meaning binding and k_{off} meaning unbinding we can calculate our parameter values. By using this differential equation of protein-protein docking rate we can realize that at equilibrium the amount of reactants and products will be equal leading to a equilibrium value of 0. With K_d's setup we then get our final equation of $K_d = k_{off}/k_{on}$ that substitutes a literature estimate from Schreiber et al's protein association kinetics to get a final K_{off} value [20].

2.1. Dosing

I model 3 different dosing paradigms for miR378: a bolus dose, pulse dosing, and loading + maintenance dosing. The bolus dose involves one singular injection, which we model as a single influx of 25000 molecules. Bolus doses are used to flood systems, increasing uptake across biological barriers and crossing the therapeutic threshold in a single pulse, immediately initiating therapeutic effect. They are also pharmacokinetically calculated as with the formula "Loading Dose $= (V_d \cdot C_{target})/F$" allowing precise dosing. (V_d = volume of distribution, C_{target} = desired plasma level, F = bio availability. These variables act as placeholders, as V_d acts as a measurable number, C_{target} value would be tested via clinical trials with tissue markers for accuracy, and F would be measured with an intravenous route. Yao et al conducted an experiment testing an inhibitor of atrial exosome release called GW4869 by administering it intravenously to test its pro-fibrotic effects, resulting in its success with quantifiable results utilizing western blotting, nanoparticle tracking analysis, etc. In this aspect of how GW4869 can bring out its effects intravenously, inverse effects can occur with miR378 [21]. A multiple pulse injection is administered through a series of timed intervals. In this case, we've decided to inject an amount of 5000 molecules every week for a repeat cycle of 4, meaning that once every week, a dosage of 5000 molecules will be injected for 5 weeks. Many of our body functions follow our circadian rhythms which is where the aspect of chronopharmacotherapy with multiple pulse is very optimal for conditions like myocardial infarction resulting from fibrosis. Factors like biological tolerance and degradation factors that can occur are what support the aspect of multiple pulse injections [22]. Finally, the last type of dosage used was a loading dose followed by maintenance doses. In this model, we combine the aspects of both types of drugs. In the loading dose, we inject an amount of 1000 molecules, followed by maintenance doses, injecting 500 molecules every hour. A paper testing Levosimendan's effects on heart failure administered single bolus infusions as a loading dose followed by smaller continuous infusions over 24 hours, finding success in reducing heart failure through biomarkers [23]. To verify the starting effects of the drug, a side-by-side plot was created to evaluate the effects of the different cytosol component amounts, independently testing the effects of each dosage type. The root cause of many cardiac conditions has been diagnosed, but now the use of dosage as an independent variable allows us to specify even further the most effective treatment for collagen-related heart conditions.

3. Results

In the 3 doses, the results of the amount of collagen I were tracked over the course of 800 hours (33.3 days) in the unit of molecules. The results of the experiment simulated that the loading + maintenance dosage have the same results as the bolus dose which are the most successful of decreasing collagen production over the course of the 800 hours in an exponential pattern while the pulsed dosage ended up being the least effective with decreases and increases eventually spiking up and dosage effectiveness wearing off at 700 hours of the drug being administered via the simulation. The implication of both bolus dosage and load + maintenance having the same effects on collagen production is in a clinical perspective. Loading and maintenance dosages are more expensive and harder to maintain for patients compared to bolus doses that are single injections, less effort and easier to track in patient progress. Thus, regardless of the same results, bolus doses tend to be more effective for doctors when treating fibrosis.

3.1. Baseline Fibrotic Conditions

This illustrates the exponential rate of collagen production in fibrotic conditions over the course of 800 hours and is what is used a regulation to see the extent of dosage effects (Fig 7).
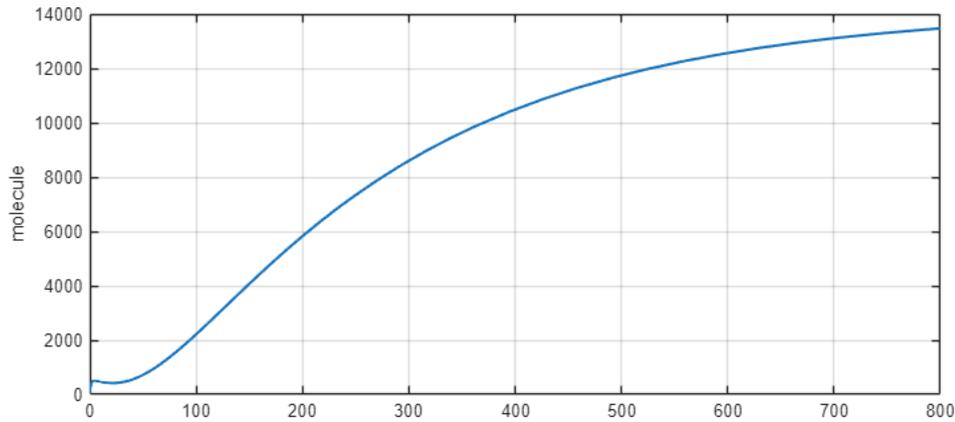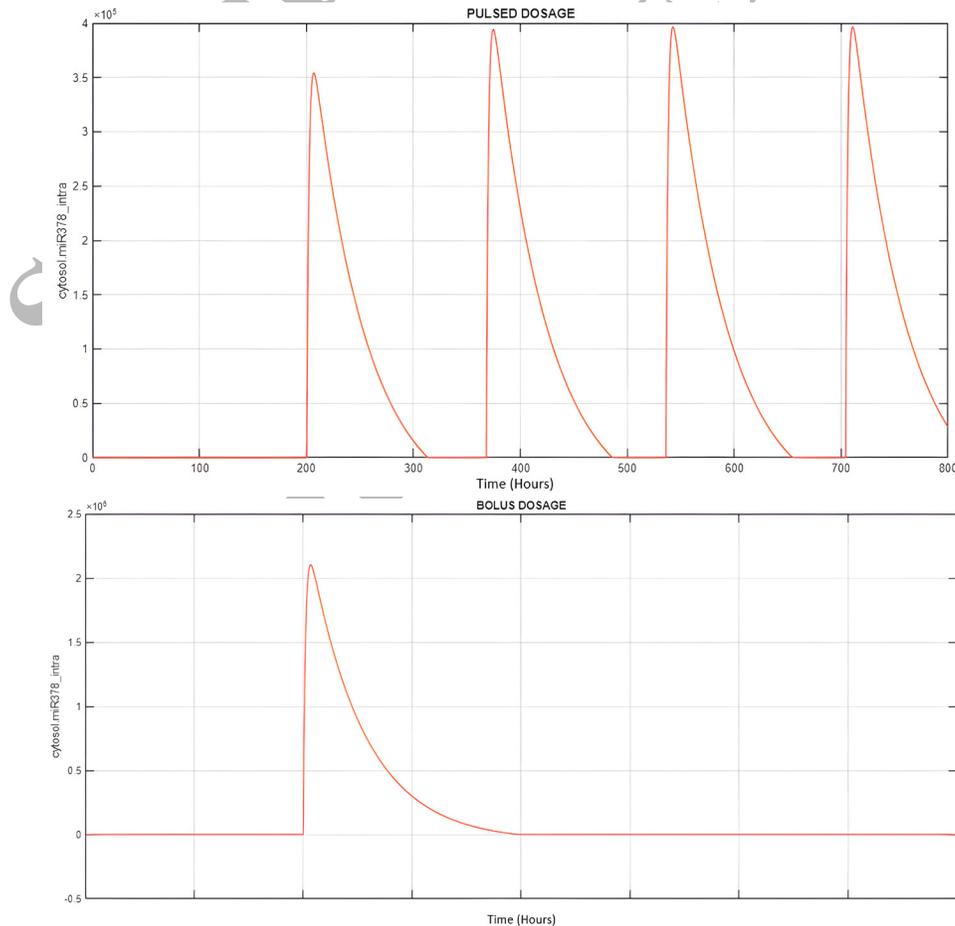

Figure 8: Fibrotic Base Conditions of CF

3.2. Pharmacokinetic Results

In the Bolus dose, the start time is 200 hours and a strong exponential decline in collagen over the course of 800 hours reaching a stagnant value of close to 0. This shows that bolus doses are strongly effective in treating fibrosis (Fig 8).

LOADING + MAINTENANCE DOSAGE

3.3. Pharmacodynamic Results

4. Limitations

This computational biologic model to stop cardiac fibrosis has many limitations due to its theoretical nature. First, species, reactions, and parameters are simplified to simplify simulation results and model direct results to different dosage methods. To clinically model an accurate TGF-β pathway response over the course of 800 hours is impossible due to the aspect of stochasticity. The next limitation of this model is that there are various values of each species that are hard to accurately represent because accurately tracking amounts of molecules and rates of biological processes varies from patient to patient, as well as the fact that clinical research hasn't explicitly mentioned the amounts. Due to these values in this model, they are sometimes estimated in order to maintain functional simulation of the model without disrupting the processes that are occurring. Additionally in H Dock protein docking the RSMD values ¿5 angstroms represent greater chance of error and limits modeling accuracy which is literature and model refitting was implemented rather biophysical modeling support.

5. Future Avenues

There are 2 aspects of exosome drug delivery that are important to touch on: the delivery method as well as the process of embodying miR-378 into exosomes. The most viable option to be able to test the effects of this exosome drug delivery for humans would be in vitro. To perform an in-vitro fibroblast assay, we must extract cardiac tissue and exosomes. We can extract exosomes from dermal stem/progenitor cells (DSPCS) and aliquoting them for future manipulation of inserting miR-378 for the drug delivery. There are multiple methods for loading miR-378 into exosomes, we can approach it by using electroporation, sonication, freeze-thaw cycles and many others. We can now approach the final steps of this process. Based on this computational model the most successful drug delivery method is continuous infusion compared to bolus doses and pulsed doses, but they can also be tested in cell plates. By injecting the modified exosomes into the cell plates through the different methods, it's possible to analyze which process reduces the excessive collagen production that occurs when MMP-TIMP

complexes aren't functioning to their full potential. Based on the data that arises from these in-vitro tests, it is possible to eventually reach avenues for testing the effects of drug delivery on humans. The success of the reduction of collagen can bypass conditions such as atrial fibrosis and fibrillation, myocardial infarctions, and many other conditions that are caused by the blockage of excess collagen. Overall, very little has been discovered about exosomes and their potential regarding its mechanisms, how it differentiates and structurally wise. This problem is also applicable to the vast processes involved in collagen synthesis and control. There are many speculative theories and research papers illustrating various miRNA strands that are pro-fibrosis, paracrine signaling related miRNA inside exosomes that communicate uptake site directions and strands are specifically used for reducing fibrosis related to different heart conditions originating from different cells such as endothelial cells, cardiomyocytes, mesenchymal stromal cells, macrophages etc. Much more research on the target pathways, functions of different exosomal contents and the kinetic mechanisms of exosomes are needed for future success.

6. Conclusion

The production of collagen in the cardiac interstitium is regulated by several complexes and proteins. In this model, the focus of the TIMP-MMP malfunction is primarily centered on leading to excessive collagen production within the heart, which induces adverse effects, leading to a multitude of heart conditions. Exploration of CF therapeutics has currently been restricted to only in vivo experimentation and knockout models. In the context of future potential for treatment via in vitro, this computational model using SimBiology® simulates 3 drug delivery paradigms: bolus, pulsed, and loading + maintenance doses. These doses utilize exosomes modified with miR378, a specific strand of miRNA from cardiac tissue. Simulation is aided by thermodynamic calculations of CD63-TIMP1 and AGO2-Collagen RNA binding affinities, molecule degradation, uptake, and protein synthesis rates coercively. The results of the computational method predicted that the pulsed and bolus doses effectively reduce CF conditions the most successfully. At 800 hours, the collagen production stagnates at a close quantitative collagen molecule amount of 0 compared

to loading + maintenance dose pulse with lost efficacy around 650 hours with similar results to the alternate paradigms.

Data Availablity Statement
The full Simbiology model file consisting of parameters, species and reactions are available in the project file "TGf-B pathway model.sbproj" along with thermodynamic binding values of proteins and RNAs at https://doi.org/10.5281/zenodo.17365252.

References
1. Gulati, A., Jabbour, A., Ismail, T. F., Guha, K., Khwaja, J., Raza, S., ... & Prasad, S. K. (2013). Association of fibrosis with mortality and sudden cardiac death in patients with nonischemic dilated cardiomyopathy. *Jama, 309*(9), 896-908.
2. Piek, A., De Boer, R. A., & Silljé, H. H. W. (2016). The fibrosis-cell death axis in heart failure. *Heart failure reviews, 21*(2), 199-211.
3. Yellon, D. M., & Davidson, S. M. (2014). Exosomes: nanoparticles involved in cardioprotection?. *Circulation research, 114*(2), 325-332.
4. Tang, X., Leng, M., Tang, W., Cai, Z., Yang, L., Wang, L., ... & Guo, J. (2024). The roles of exosome-derived microRNAs in cardiac fibrosis. *Molecules, 29*(6), 1199.
5. Weber, K. T., Sun, Y., Tyagi, S. C., & Cleutjens, J. P. (1994). Collagen network of the myocardium: function, structural remodeling and regulatory mechanisms. *Journal of molecular and cellular cardiology, 26*(3), 279-292.
6. Pogontke, C., Guadix, J. A., Ruiz-Villalba, A., & Pérez-Pomares, J. M. (2019). Development of the myocardial interstitium. *The Anatomical Record, 302*(1), 58-68.
7. Dzeshka, M. S., Lip, G. Y., Snezhitskiy, V., & Shantsila, E. (2015). Cardiac fibrosis in patients with atrial fibrillation: mechanisms and clinical implications. *Journal of the American College of Cardiology, 66*(8), 943-959.
8. Moz, S., Basso, D., Bozzato, D., Galozzi, P., Navaglia, F., Negm, O. H., ... & Plebani, M. (2016). SMAD4 loss enables EGF, TGFβ1 and S100A8/A9 induced activation of critical pathways to invasion in human pancreatic adenocarcinoma cells. *Oncotarget, 7*(43), 69927.
9. Wang, W., Gao, W., Zhu, Q., Alasbahi, A., Seki, E., & Yang, L. (2021). TAK1: a molecular link between liver inflammation, fibrosis, steatosis, and carcinogenesis. *Frontiers in cell and developmental biology, 9*, 734749.
10. Yuan, J., Liu, H., Gao, W., Zhang, L., Ye, Y., Yuan, L., ... & Zou, Y. (2018). MicroRNA-378 suppresses myocardial fibrosis through a paracrine mechanism at the early stage of cardiac hypertrophy following mechanical stress. *Theranostics, 8*(9), 2565.
11. Lee, M. K., Pardoux, C., Hall, M. C., Lee, P. S., Warburton, D., Qing, J., ... & Derynck, R. (2007). TGF-β activates Erk MAP kinase signalling through direct phosphorylation of ShcA. *The EMBO journal, 26*(17), 3957-3967.
12. Weber, B., & Hoerstrup, S. P. (2011). *Regenerating heart valves. In Regenerating the heart: Stem cells and the cardiovascular system* (pp. 403-442). Totowa, NJ: Humana Press.
13. Jungers, C. F., & Djuranovic, S. (2022). Modulation of miRISC-mediated gene silencing in eukaryotes. *Frontiers in molecular biosciences, 9*, 832916.
14. Ziemys, A., Yokoi, K., & Kojic, M. (2015). Capillary collagen as the physical transport barrier in drug delivery to tumor microenvironment. *Tissue Barriers, 3*(3), e1037418.
15. Huang, S. Y., & Zou, X. (2008). An iterative knowledge-based scoring function for protein–protein recognition. *Proteins: Structure, Function, and Bioinformatics, 72*(2), 557-579.
16. Huang, S. Y., & Zou, X. (2014). A knowledge-based scoring function for protein-RNA interactions derived from a statistical mechanics-based iterative method. *Nucleic acids research, 42*(7), e55-e55.
17. Yan, Y., Zhang, D., Zhou, P., Li, B., & Huang, S. Y. (2017). HDOCK: a web server for protein–protein and protein–DNA/RNA docking based on a hybrid strategy. *Nucleic acids research, 45*(W1), W365-W373.
18. Taylor, E. S., Pol-Fachin, L., Lins, R. D., & Lower, S. K. (2017). Conformational stability of the epidermal growth factor (EGF) receptor as influenced by glycosylation, dimerization and EGF hormone binding. *Proteins: Structure, Function, and Bioinformatics, 85*(4), 561-570.
19. Yan, Y., Tao, H., He, J., & Huang, S. Y. (2020). The HDOCK server for integrated protein–protein docking. *Nature protocols, 15*(5), 1829-1852.
20. Schreiber, G., Haran, G., & Zhou, H. X. (2009). Fundamental aspects of protein− protein association kinetics. *Chemical reviews, 109*(3), 839-860.
21. Yao, Y., He, S., Wang, Y., Cao, Z., Liu, D., Fu, Y., ... & Zhao, Q. (2021). Blockade of exosome release suppresses atrial fibrillation by alleviating atrial fibrosis in canines with prolonged atrial pacing. *Frontiers in Cardiovascular Medicine, 8*, 699175.
22. Reddy, J. R. K., Jyothsna, M. V., Saleem, T. M., & Chetty, C. M. S. (2009). Review on: pulsatile drug delivery systems. *Journal of Pharmaceutical Sciences and Research, 1*(4), 109.
23. Tasal, A., Demir, M., Kanadasi, M., Bacaksiz, A., Vatankulu, M. A., Sahin, D. Y., ... & Acarturk, E. (2014). Comparison of single-dose and repeated levosimendan infusion in patients with acute exacerbation of advanced heart failure. *Medical science monitor: international medical journal of experimental and clinical research, 20*, 276.